ORIGINAL INVESTIGATION

The additive effects of type 2 diabetes mellitus on left ventricular deformation and myocardial perfusion in essential hypertension: a 3.0 T cardiac magnetic resonance study

Xue-Ming Li[1,2†], Li Jiang[1†], Ying-Kun Guo[3], Yan Ren[4], Pei-Lun Han[1], Li-Qing Peng[1], Rui Shi[1], Wei-Feng Yan[1] and Zhi-Gang Yang[1*]

Abstract

Background: Type 2 diabetes mellitus (T2DM) increases the risks of heart failure and mortality in patients with hypertension, however the underlying mechanism is unclear. This study aims to investigate the impact of coexisting T2DM on left ventricular (LV) deformation and myocardial perfusion in hypertensive individuals.

Materials and methods: Seventy hypertensive patients without T2DM [HTN(T2DM−)], forty patients with T2DM [HTN(T2DM+)] and 37 age- and sex-matched controls underwent cardiac magnetic resonance examination. Left ventricular (LV) myocardial strains, including global radial (GRPS), circumferential (GCPS) and longitudinal peak strain (GLPS), and resting myocardial perfusion indices, including upslope, time to maximum signal intensity (TTM), and max signal intensity (MaxSI), were measured and compared among groups by analysis of covariance after adjusting for age, sex, body mass index (BMI) and heart rate followed by Bonferroni's post hoc test. Backwards stepwise multivariable linear regression analyses were performed to determine the effects of T2DM on LV strains and myocardial perfusion indices in patients with hypertension.

Results: Both GRPS and GLPS deteriorated significantly from controls, through HTN(T2DM−), to HTN(T2DM+) group; GCPS in HTN(T2DM+) group was lower than those in both HTN(T2DM−) and control groups. Compared with controls, HTN(T2DM−) group showed higher myocardial perfusion, and HTN(T2DM+) group exhibited lower perfusion than HTN(T2DM−) group and controls. Multiple regression analyses considering covariates of systolic blood pressure, age, sex, BMI, heart rate, smoking, indexed LV mass and eGFR demonstrated that T2DM was independently associated with LV strains (GRPS: $p = 0.002$, model $R^2 = 0.383$; GCPS: $p < 0.001$, model $R^2 = 0.472$; and GLPS: $p = 0.002$, model $R^2 = 0.424$, respectively) and perfusion indices (upslope: $p < 0.001$, model $R^2 = 0.293$; TTM: $p < 0.001$, model $R^2 = 0.299$; and MaxSI: $p < 0.001$, model $R^2 = 0.268$, respectively) in hypertension. When both T2DM and perfusion indices were included in the regression analyses, both T2DM and TTM were independently associated with GRPS ($p = 0.044$ and

Li *et al. Cardiovasc Diabetol* (2020) 19:161

Page 2 of 10

0.017, model R^2 = 0.390) and GCPS (p = 0.002 and 0.001, model R^2 = 0.424), and T2DM but not perfusion indices was independently associated with GLPS (p = 0.002, model R^2 = 0.424).

Conclusion: In patients with hypertension, T2DM had an additive deleterious effect on subclinical LV systolic dysfunction and myocardial perfusion, and impaired myocardial perfusion by coexisting T2DM was associated with deteriorated LV systolic dysfunction.

Keywords: Hypertension, Type 2 diabetes mellitus, Left ventricular strains, Perfusion, Magnetic resonance imaging

Introduction

Given their common risk factors, essential hypertension and type 2 diabetes mellitus (T2DM) frequently coexist. Approximately 70% of patients with T2DM have hypertension, and the development of T2DM is almost 2.5 times more likely in patients with precedent hypertension [1, 2]. It is well known that both hypertension and T2DM are well-established risk factors for cardiovascular disease morbidity and mortality regardless of the presence of each factor [3]. In addition, T2DM in hypertensive patients further increases the risks of heart failure and all-cause and cardiovascular mortality [4, 5]. Once established, heart failure is associated with worse clinical outcomes. Therefore, early detection of subclinical left ventricular (LV) myocardial dysfunction allows for earlier intervention, which may potentially prevent heart failure and improve patient outcomes.

Cardiac magnetic resonance (CMR) has less shortcomings of echocardiography, such as acoustic window limitations, low spatial resolution and high operator dependency, and can evaluate cardiac anatomy and function as well as myocardial perfusion in a single examination [6]. The commonly used global volumetric measurement of left ventricular ejection fraction (LVEF) cannot provide a detailed assessment of cardiac mechanics, and it has been demonstrated to be an insensitive and late marker of contractile impairment [7]. Recently, CMR feature tracking using routinely acquired cine images has become a more sensitive technique for evaluating global and regional myocardial deformation as an indicator of subclinical myocardial dysfunction [8]. In addition, CMR-derived first-pass myocardial perfusion has been increasingly used to noninvasively evaluate myocardial microcirculation function with high reproducibility [9, 10].

Although limited echocardiographic studies have observed more severe subclinical systolic dysfunction in patients with coexisting hypertension and T2DM than in those with T2DM alone [11–14], none have evaluated the impact of T2DM on LV deformation and myocardial microcirculation function in patients with hypertension. Accordingly, the aim of this study was to investigate the impact of coexisting T2DM on subclinical LV systolic dysfunction and myocardial microcirculation function using CMR in patients with hypertension.
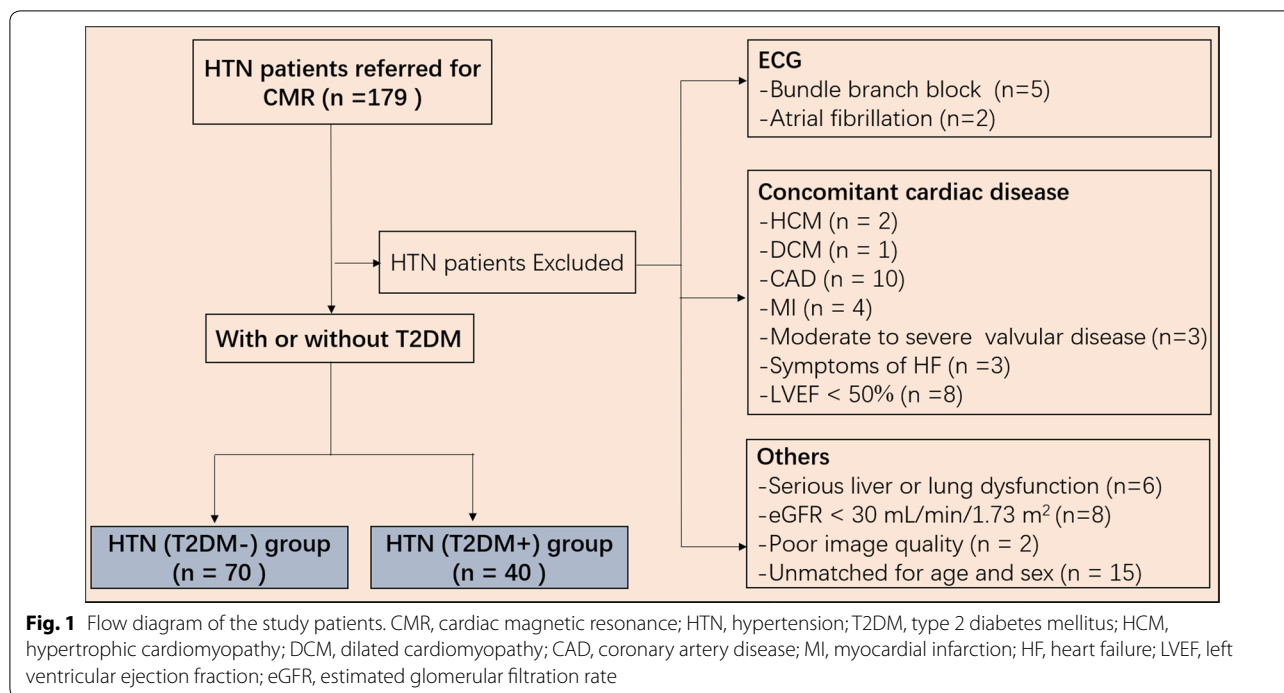
Materials and methods

Study population

From January 2016 to January 2020, 179 Adult Chinese Han race essential hypertensive patients with or without T2DM [HTN(T2DM+) and HTN(T2DM−), respectively] who underwent CMR at our institution were consecutively included. Hypertension was defined as a clinical systolic blood pressure (SBP) ≥ 140 mmHg and/or a diastolic blood pressure (DBP) ≥ 90 mmHg or a history of antihypertensive medications. The diagnosis of T2DM was based on the current American Diabetes Association guideline recommendations [15]. The exclusion criteria (Fig. 1) included patients with symptoms of heart failure (n = 3), LVEF < 50% (n = 8), known coronary artery disease (n = 10), myocardial infarction (n = 4), moderate to severe valvular disease (n = 3), cardiomyopathy (n = 3), bundle branch block (n = 5), atrial fibrillation (n = 2), serious liver and lung dysfunction (n = 6), estimated glomerular filtration rate (eGFR) < 30 mL/min/1.73 m^2 (n = 8) and poor image quality (n = 2). In addition, patients unmatched for age and sex (n = 15) were also excluded. Finally, 110 patients including 70 (35 men and 35 women; mean age, 55.0 ± 14.1 years) and 40 (20 men and 20 women; mean age, 55.7 ± 9.8 years) age- and sex-matched patients with HTN (T2DM−) and HTN (T2DM+), were eligible for this study. Another 37 healthy individuals (18 men and 19 women; mean age, 54.2 ± 10.5 years) matched for age and sex were selected from our healthy volunteer database to serve as the control group, and they underwent the same CMR examination.

This study was approved by the Biomedical Research Ethics Committee of our hospital and conducted in accordance with the Declaration of Helsinki (2013 EDITION).

CMR protocol

All the CMR examinations were performed using a 3.0 T whole-body scanner (Trio Tim; Siemens Medical Solutions, Erlangen, Germany) in the supine

Li et al. Cardiovasc Diabetol   (2020) 19:161

Page 3 of 10

Fig. 1 Flow diagram of the study patients. CMR, cardiac magnetic resonance; HTN, hypertension; T2DM, type 2 diabetes mellitus; HCM, hypertrophic cardiomyopathy; DCM, dilated cardiomyopathy; CAD, coronary artery disease; MI, myocardial infarction; HF, heart failure; LVEF, left ventricular ejection fraction; eGFR, estimated glomerular filtration rate

position. Data acquisition was performed with a standard ECG-triggering device that monitored each subject's dynamic ECG changes during the end-inspiratory breath hold period. A balanced steady-state free precession (bSSFP) sequence (repetition time [TR]: 39.34 ms, echo time [TE]: 1.22 ms, flip angle: 40°, slice thickness: 8 mm, field of view [FOV]: 250×300 mm, and matrix size: 208×139) was used to acquire 8 - 12 continuous cine images from the base to the apex in the short-axis view, as well as vertical LV two- and four-chamber cine images in the long-axis view. For perfusion imaging, a dose of 0.2 mL/kg gadobenate dimeglumine (MultiHance 0.5 mmol/mL; Bracco, Milan, Italy) was injected into the right antecubital vein with a power injector (Stellant, MEDRAD, Indianola, PA, USA) at a flow rate of 2.5–3.0 mL/s, followed by 20 mL of saline. Rest first-pass perfusion images were acquired in three standard short-axis slices (basal, middle, and apical) and in one four-chamber view slice by inversion recovery prepared echo-planar imaging sequence (TR/TE: 163.0/1.12 ms, flip angle: 10°, slice thickness: 8 mm, FOV: 360 mm $\times$ 270 mm, and matrix size: 256×192). To exclude myocardial infarction, late gadolinium enhancement (LGE) images were acquired by segmented-turbo-FLASH–phase-sensitive inversion recovery (PSIR) sequences (TR/TE: 750 ms/1.18 ms; flip angle: 40°, slice thickness: 8 mm, FOV: 400×270 mm,
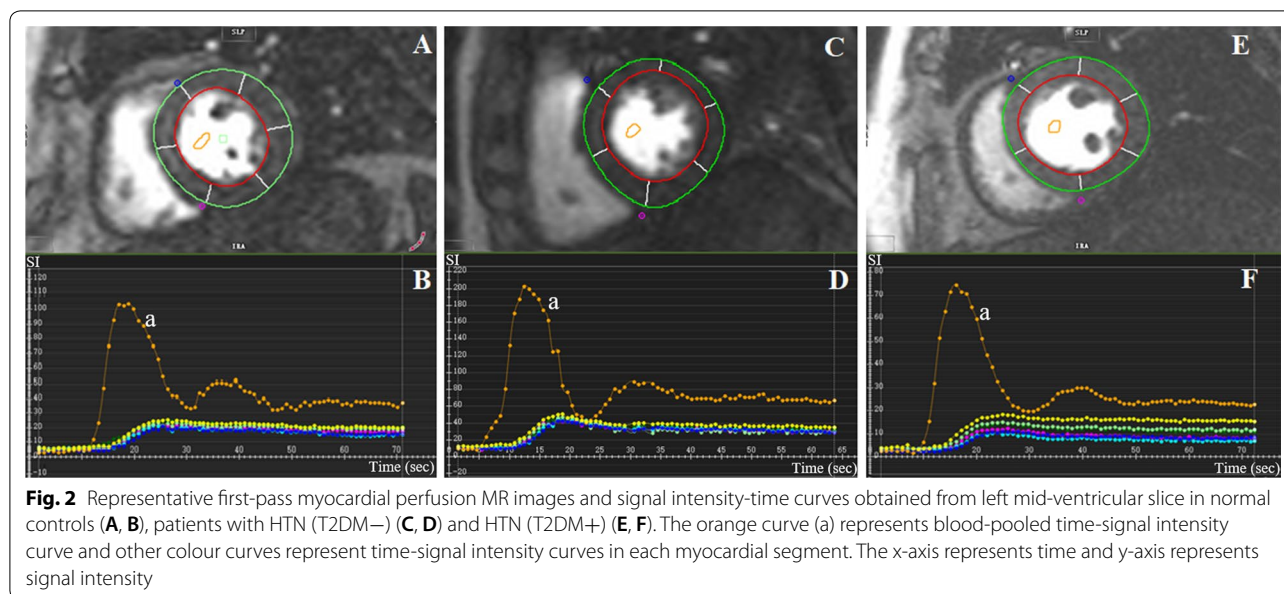
and matrix size: 256×148) 10–15 min after contrast administration.

CMR data analysis

CMR images were evaluated using offline commercially available software (cvi42, v. 5.10.2; Circle Cardiovascular Imaging, Calgary, Canada) by two radiologists with more than 3 years of CMR experience, who were blinded to the clinical data.

The endocardial and epicardial contours of the LV myocardium on the short-axis cine images were manually traced at the end-diastolic and end-systolic phases in the cvi42 short-3D module. Then, LV mass at end-diastole, LV end-diastolic volume (LVEDV), LV end-systolic volume (LVESV), LVEF, stroke volume and cardiac index were computed automatically. The trabeculae and papillary muscles were excluded from the LV mass and included in the LV cavity. LV mass, LVEDV and LVESV indexed for body surface area (BSA) (LVMI, LVEDVI and LVESVI, respectively) were calculated using the Mosteller formula [16]. In addition, LV remodeling index, calculated as LVM/LVEDV, was included for analysis.

The LV global radial (GRPS), circumferential (GCPS) and longitudinal peak strain (GLPS) were obtained by manually delineating the endocardium and epicardium of the cine images at the end-diastole from the short-axis and long-axis two- and four-chamber slice views in the tissue tracking module. Strain was depicted as relative

Li *et al. Cardiovasc Diabetol* (2020) 19:161

Page 4 of 10

Fig. 2 Representative first-pass myocardial perfusion MR images and signal intensity-time curves obtained from left mid-ventricular slice in normal controls (**A**, **B**), patients with HTN (T2DM−) (**C**, **D**) and HTN (T2DM+) (**E**, **F**). The orange curve (a) represents blood-pooled time-signal intensity curve and other colour curves represent time-signal intensity curves in each myocardial segment. The x-axis represents time and y-axis represents signal intensity

lengthening, shortening and thickening of the myocardium from end diastole (reference phase).

For the evaluation of first-pass myocardial perfusion (Fig. 2), the endocardium and epicardium and a region of interest drawn in the LV chamber were manually determined in the first-pass perfusion images (basal, middle and apical). Then, signal intensity-time curves were generated for the blood pool and each myocardial segment based on the 16-segment heart model. Consequently, semiquantitative segmental perfusion indices including the upslope, time to maximum signal intensity (TTM), and max signal intensity (MaxSI) were acquired automatically, and the global first-pass myocardial perfusion indices for each subject were calculated by averaging the regional values of the 16 myocardial segments. In addition, the presence of LGE was visually evaluated by the two radiologists with consensus.

Reproducibility of LV myocardial strain and perfusion

Intra- and inter-observer variabilities for the LV global myocardial strain and perfusion indices were analyzed in 30 random cases including 20 HTN patients and 10 controls. To determine the intra-observer variability, one observer (XM. L) evaluated the same subjects on two separate measurements 1 month apart. For the inter-observer variability evaluation, a second investigator (L. J) who was blinded to the first observer's results and clinical data reanalyzed the measurements.

Statistical analysis

Categorical variables are presented as frequencies (percentages) and were compared using Chi square tests.

Continuous variables were evaluated for normality distribution by the Shapiro–Wilk test and are expressed as the mean ± standard deviation (SD). One-way analysis of variance (one-way ANOVA) was used to compare the baseline characteristics among the normal and HTN groups. Comparisons of the CMR-derived parameters between different groups were evaluated by analysis of covariance (ANCOVA) after adjusting for age, sex, body mass index (BMI) and heart rate followed by Bonferroni's post hoc test. Pearson's correlation coefficient was used to determine the correlation between LV myocardial strain and first-pass myocardial perfusion indices in HTN. Backwards stepwise multivariable linear regression analyses were performed to determine the predictors for LV strains and myocardial perfusion indices in the whole population and patients with HTN. Inter- and intra-observer agreements were determined by the evaluation of intraclass correlation coefficients (ICCs). All analyses were performed in SPSS version 21 (IBM, Armonk, New York, USA), and a two-tailed $p < 0.05$ was considered significant.

Results

Baseline characteristics

The main clinical characteristics of the study participants are summarized in Table 1. Age, BSA, heart rate, plasma triglycerides, total cholesterol, high-density lipoprotein cholesterol, low-density lipoprotein cholesterol and eGFR were not significantly different between the observed groups (all $p > 0.05$), except for a higher BMI in both the HTN (T2DM−) and HTN (T2DM+) groups than in the control group (all $p < 0.01$). As expected,

Li *et al. Cardiovasc Diabetol*   (2020) 19:161

Page 5 of 10

Table 1 Baseline characteristics of the study cohort

	Controls	HTN (T2DM−)	HTN (T2DM+)
	n = 37	n = 70	n = 40
Demographics			
Age (years)	54.2 ± 10.5	55.0 ± 14.1	55.7 ± 9.8
Male; n (%)	19 (51.4)	35 (50.0)	20 (50.0)
BMI (kg/m²)	23.00 ± 2.74	24.76 ± 3.01*	25.04 ± 2.20*
BSA (kg/m²)	1.70 ± 0.18	1.71 ± 0.18	1.74 ± 0.16
Smoking, n (%)	0	27 (38.6)	12 (30.0)
Laboratory data			
Fasting blood glucose (mmol/L)	5.61 ± 1.67	5.30 ± 1.01	7.98 ± 2.67[§]
Plasma triglycerides (mmol/L)	1.34 ± 0.53	1.76 ± 1.28	1.92 ± 1.64
Total cholesterol (mmol/L)	4.71 ± 1.04	4.39 ± 1.04	4.22 ± 0.80
HDL (mmol/L)	1.44 ± 0.40	1.40 ± 1.12	1.21 ± 0.28
LDL (mmol/L)	2.82 ± 0.97	2.52 ± 0.81	2.38 ± 0.67
eGFR (mL/min/1.73 m²)	98.4 ± 14.5	93.6 ± 18.8	90.2 ± 18.8
Hemodynamic variables			
Heart rate (beats/min)	70.1 ± 9.9	72.9 ± 16.7	71.5 ± 10.1
SBP (mmHg)	114.2 ± 13.2	141.1 ± 19.5*	138.7 ± 14.5*
DBP (mmHg)	71.6 ± 8.5	87.7 ± 16.5*	84.6 ± 9.6*
HTN treatment			
ACEI/ARB, n (%)	0	28 (40.0)	14 (35.0)
Beta-blocker, n (%)	0	27 (38.6)	16 (40.0)
Calcium channel blocker, n (%)	0	39 (55.7)	19 (47.5)
Diuretics, n (%)	0	10 (14.3)	6 (15.0)
Diabetes treatment			
Oral, n (%)	0	0	33 (82.5)
Insulin, n (%)	0	0	7 (17.5)

The values are the mean ± SD, Numbers in the brackets are percentages

HTN, hypertension; T2DM, type 2 diabetes mellitus; BMI, body mass index; BSA, body surface area; HDL, high-density lipoprotein cholesterol; LDL, low-density lipoprotein cholesterol; eGFR, estimated glomerular filtration rate; ACEI, angiotensin converting enzyme inhibitor; ARB, angiotensin II receptor blocker

* $p < 0.005$ versus controls

[§] $p < 0.001$ versus controls and HTN (T2DM−) group

fasting blood glucose was significantly higher in the HTN (T2DM+) group than in the HTN (T2DM−) group and control group (all $p < 0.001$). In addition, both SBP and DBP were significantly higher in the hypertensive groups than in the control group (all $p < 0.001$).

Comparison of CMR findings among groups

The CMR findings for the observed groups are shown in Table 2. The LVMI ($p < 0.001$ and = 0.005, respectively) and LV remodeling index ($p < 0.001$ and = 0.040, respectively) in both the HTN (T2DM−) and HTN (T2DM+) groups were significantly higher than those in the control group, whereas the LVEDVI, LVESVI, LVEF, stroke volume and cardiac index were not significantly different among the groups (all $p > 0.05$).

The LV GRPS and GLPS (all $p < 0.05$ and 0.027, respectively) declined significantly from controls, through HTN (T2DM−) group, to HTN(T2DM+) group. Compared with the control group, the LV GCPS was decreased in the HTN(T2DM+) group ($p = 0.005$) but preserved in the HTN (T2DM−) group.

Compared with the control group, higher myocardial perfusion was observed in the HTN (T2DM−) group as supported by increased upslope ($p = 0.023$) and MaxSI ($p = 0.005$), and lower myocardial perfusion was demonstrated in the HTN (T2DM+) group as supported by decreased upslope ($p = 0.036$) and increased TTM ($p = 0.038$). In addition, the HTN (T2DM+) group exhibited worse myocardial perfusion than the HTN (T2DM−) group, which was supported by a reduced upslope and MaxSI (all $p < 0.001$) and increased TTM (all $p = 0.001$) values.

Li *et al. Cardiovasc Diabetol*   (2020) 19:161

Page 6 of 10

Table 2 Comparisons of CMR findings between controls, HTN (T2DM−) group and HTN (T2DM+) group after adjustment for age, sex, BMI and heart rate

	Controls n = 37	HTN (T2DM−) n = 70	HTN (T2DM+) n = 40	P value
LV geometry and function				
LVMI (g/m²)	44.55 ± 8.06	58.07 ± 16.02*	55.22 ± 13.22*	< 0.001
LVEDVI (mL/m²)	75.92 ± 12.42	78.26 ± 17.00	76.95 ± 13.51	0.223
LVESVI (mL/m²)	28.51 ± 7.62	28.65 ± 10.71	29.39 ± 9.02	0.437
LVEF (%)	62.85 ± 6.20	63.84 ± 7.04	63.00 ± 7.66	0.408
Stroke volume (mL)	78.09 ± 12.04	83.99 ± 21.10	80.18 ± 14.66	0.082
Cardiac index (L/min/m²)	3.27 ± 0.60	3.70 ± 0.86	3.37 ± 0.72	0.068
LV remodeling index (g/mL)	0.60 ± 0.12	0.75 ± 0.17*	0.73 ± 0.18*	0.001
Myocardial strain				
GRPS (%)	38.98 ± 8.14	36.57 ± 10.81*	31.77 ± 10.91*§	< 0.001
GCPS (%)	− 21.44 ± 2.74	− 21.41 ± 3.10	− 19.88 ± 3.59*§	0.004
GLPS (%)	− 14.94 ± 2.42	− 13.14 ± 2.66*	− 11.75 ± 3.69*§	< 0.001
Myocardial perfusion				
Upslope	2.73 ± 1.17	3.30 ± 1.29*	1.83 ± 0.74*§	< 0.001
TTM (s)	26.90 ± 10.15	23.30 ± 8.78	31.65 ± 12.57*§	0.002
MaxSI	23.03 ± 8.03	27.10 ± 9.64*	18.05 ± 6.78§	< 0.001

HTN, hypertension; T2DM, type 2 diabetes mellitus;LV, left ventricular; M, mass; EDV, end diastolic volume; ESV, end systolic volume; I, indexed to BSA; EF, ejection fraction; GRPS, global radial peak strain; GCPS, global circumferential peak strain; GLPS, global longitudinal peak strain; TTM, time to maximum signal intensity; MaxSI, max signal intensity

* *p* < 0.05 versus controls

§ *p* < 0.05 versus HTN (T2DM−) group

Association among LV strain, myocardial perfusion and clinical variables in the whole population

Multivariable linear regression analyses demonstrated that considering the covariates of SBP, age, sex, BMI, BSA, heart rate, SV and LVM, both hypertension and T2DM were independently associated with LV GLPS ($\beta = 1.469$ and 1.569, $p = 0.006$ and 0.003, model $R^2 = 0.467$), and T2DM but not hypertension was independently associated with LV GCPS and GRPS ($\beta = 1.553$, $p = 0.002$, model $R^2 = 0.442$ and $\beta = − 5.493$, $p = 0.001$, model $R^2 = 0.425$, respectively). In addition, both hypertension and T2DM were independently associated with upslope ($\beta = 0.608$ and $− 1.437$, $p = 0.009$ and < 0.001, model $R^2 = 0.293$) and MaxSI ($\beta = 4.346$ and $− 9.223$, $p = 0.014$ and < 0.001, model $R^2 = 0.232$), and T2DM but not hypertension was independently associated with TTM ($\beta = 5.878$, $p = 0.001$, model $R^2 = 0.371$).

Association between myocardial strain and first-pass myocardial perfusion in hypertension

LV GRPS, GCPS and GLPS were significantly associated with upslope and TTM, whereas they were not associated with MaxSI (Table 3).

Multivariable linear regression analyses (Table 4) revealed that considering the covariates of SBP, age, sex, BMI, heart rate, smoking, LVMI and eGFR, T2DM was independently associated with LV strains (GRPS: $\beta = − 6.178$, $p = 0.002$, model $R^2 = 0.383$; GCPS: $\beta = 2.314$, $p < 0.001$, model $R^2 = 0.472$; and GLPS: $\beta = 1.685$, $p = 0.002$, model $R^2 = 0.424$, respectively) and first-pass myocardial perfusion indices (upslope: $\beta = − 1.448$, $p < 0.001$, model $R^2 = 0.293$; TTM: $\beta = 8.188$, $p < 0.001$, model $R^2 = 0.299$; and MaxSI: $\beta = − 9.325$, $p < 0.001$, model $R^2 = 0.268$, respectively). Furthermore, when both T2DM and all the perfusion indices were

Table 3 Correlation of LV myocardial strain with first-pass perfusion indices in all patients with hypertension

	Upslope		TTM (s)		Max SI	
	r	p value	r	p value	r	p value
GRPS (%)	0.292	0.003	− 0.355	<0.001	0.092	0.362
GCPS (%)	− 0.226	0.024	0.390	<0.001	− 0.067	0.508
GLPS (%)	− 0.299	0.002	0.279	0.005	− 0.144	0.152

Li *et al. Cardiovasc Diabetol*   (2020) 19:161

Page 7 of 10

Table 4 Multivariable association of diabetes with first-pass myocardial perfusion indices or LV strains in all patients with hypertension adjusted for SBP, age, sex, BMI, heart rate, smoking, LVMI and eGFR

Model 1	TTM		Upslope		MaxSI	
	Coefficient (95% CI)	R^2	Coefficient (95% CI)	R^2	Coefficient (95% CI)	R^2
Diabetes	8.188 (4.063 to 12.312) *	0.299	− 1.448 (− 1.952 to − 0.944) *	0.293	− 9.325 (− 13.117 to − 5.533) *	0.268
	GRPS		GCPS		GLPS	
	Coefficient (95% CI)	R^2	Coefficient (95% CI)	R^2	Coefficient (95% CI)	R^2
Model 2						
Diabetes	− 6.178 (− 10.059 to − 2.297)*	0.383	2.314 (1.231 to 3.398)*	0.472	1.685 (0.621 to 2.750)*	0.424
Model 3						
Diabetes	− 4.233 (− 8.343 to − 0.123)*	0.390	1.868 (0.718 to 3.018)*	0.495	1.685 (0.621 to 2.750*	0.424
TTM	− 0.221 (− 0.401 to − 0.041)*		0.054 (0.001 to 0.107)*		–	
Upslope	–		–		–	
MaxSI	–		–		–	

Abbreviation of SBP, BMI and eGFR are shown in Table 1; and LVMI, LVEDVI, GRPS, GCPS, GLPS, TTM and MaxSI in Table 2

Model 1: Association between diabetes and perfusion indices

Model 2: Association between diabetes and LV strains

Model 3: Association of LV strains with diabetes and perfusion indices

* p < 0.05; values are unstandardized estimate coefficients (B) and 95% confident interval (CI)

Table 5 Intra-and inter-observer variability of LV strains and perfusion indices

	Intra-observer		Inter-observer	
	ICC	95% CI	ICC	95% CI
GRPS	0.934	0.891–0.954	0.945	0.857–0.989
GCPS	0.972	0.915–0.991	0.957	0.945–0.994
GLPS	0.938	0.878–0.988	0.938	0.852–0.978
Upslope	0.931	0.920–0.986	0.915	0.895–0.983
TTM (s)	0.912	0.905–0.975	0.891	0.840–0.932
MaxSI	0.920	0.869–0.945	0.956	0.869–0.978

Abbreviation of GRPS, GCPS, GLPS, TTM and MaxSI are shown in Table 2

ICC, intraclass correlation coefficient; CI, confidence interval

included in the regression analyses, both T2DM and TTM were independently associated with LV GRPS ($\beta = − 4.233$, $p = 0.044$; $\beta = − 0.221$, $p = 0.017$; model $R^2 = 0.390$) and LV GCPS ($\beta = 1.868$, $p = 0.002$; $\beta = 0.054$, $p = 0.001$; model $R^2 = 0.495$), and T2DM but not perfusion indices was independently associated with LV GLPS ($\beta = 1.685$, $p = 0.002$, model $R^2 = 0.424$).

Intra-observer and inter-observer variability

As demonstrated in Table 5, there were excellent intra- and inter-observer agreements in the measurement of LV global myocardial peak strain (ICC = 0.934–0.972 and 0.938–0.957, respectively) and first-pass myocardial perfusion   (ICC = 0.912–0.931   and   0.891–0.956, respectively).

Discussion

The main findings of this study are as follows: (1) hypertension impairs LV GLPS, and coexisting T2DM further deteriorates subclinical LV systolic dysfunction; (2) myocardial perfusion is increased in HTN (T2DM−) but decreased in HTN (T2DM+) patients; and (3) impaired myocardial perfusion by T2DM is associated with aggravated LV systolic dysfunction in patients with hypertension. These changes observed in our study indicate the deleterious effect of T2DM on myocardial systolic function and myocardial microcirculation function in patients with hypertension, which may contribute to the increased cardiovascular risk.

T2DM aggravate LV dysfunction in hypertension

Similar to most progressive myocardial diseases, subendocardial fibers are more vulnerable to being affected; thus, longitudinal contractile function representing as GLPS may be impaired earlier and more severely [8], as shown in previous studies with hypertension [17–19] and T2DM [13, 20–22], as well as in our patients. In hypertension, there is insulin resistance and activation of the sympathetic nervous system and renin–angiotensin–aldosterone system, which may result in diffuse myocardial fibrosis [12]. Diffuse myocardial fibrosis and hemodynamic overload-associated LV hypertrophy are more vulnerable to the involvement of subendocardial

Li *et al. Cardiovasc Diabetol*   (2020) 19:161

Page 8 of 10

fibers. In addition, studies in hypertension have found that GCPS was significantly reduced in patients with hypertrophy [17, 23]. Recent studies showed the negative effects of acute hyperglycemia on systolic LV global longitudinal strain and multilayer longitudinal and circumferential strain in asymptomatic T2DM and unfavorable subclinical reductions in global and average circumferential strain in obese adolescents with dysglycemia, which may indicate the importance of intensive blood glucose control [24, 25]. Moreover, epicardial adipose tissue may be associated with LV structural and functional abnormalities and exercise intolerance in T2DM patients with asymptomatic heart failure [26], and serum levels of omentin-1 and Zinc-α2-glycoprotein have been recently defined as the most important predictors for LV hypertrophy and LV diastolic dysfunction in T2DM patients [27]. Our study demonstrated that T2DM aggravated LV systolic dysfunction as represented by more severe impairment of GLPS and GRPS and the occurrence of impaired GCPS in the HTN (T2DM+) group, even though similar LVEF and LV geometries were observed between the hypertensive subgroups. The reason for this may be the superimposed factors that cause contractile dysfunction in T2DM, such as impairments in excitation–contraction coupling, metabolic derangements, remodeling of the extracellular matrix and abnormalities in microvasculature [28]. Nevertheless, it may be difficult to determine the exact individual contribution, since some of them are usually found together.

The combined effect of T2DM and hypertension on microvascular dysfunction

In both hypertension and T2DM, there are structural and functional abnormalities in coronary microvasculature, including hypertrophic remodeling of small arteries and arterioles, microvascular rarefaction, and functional increases in vasoconstriction due to endothelial dysfunction [2, 28, 29]. However, resting myocardial perfusion reflecting autoregulated blood flow correlates with myocardial oxygen consumption and is mainly determined by LV wall stress, myocardial contractility and heart rate [1]. Increased myocardial perfusion was observed in our HTN (T2DM−) patients, which was consistent with previous studies [30–32]. Kjaer et al. [31] demonstrated a 25% higher baseline myocardial perfusion by positron emission tomography, and Kozakova et al. [30] revealed higher resting coronary flow in the left anterior descending artery by transesophageal Doppler echocardiography. The increased resting myocardial perfusion in hypertension may reflect an adaptive mechanism, adapting to the increased oxygen demand for the heart to work under increased afterload [29, 32]. In T2DM, increased resting myocardial perfusion has been exhibited in some

previous studies [33–35], while others have reported decreased resting perfusion [20, 36]. This discrepancy may be due to different study populations, investigation modalities, and relatively modest sample sizes. Increased plasma insulin, a known vasodilator, by insulin resistance in T2DM may explain the increased myocardial perfusion at rest [34]. Additionally, glucose and lactate oxidation is inhibited, and fatty acid oxidation is increased, which may lead to more oxygen consumption, subsequently resulting in higher resting perfusion [34, 35].

To our knowledge, reports about the combined effect of hypertension and T2DM on myocardial microcirculation are still missing. We found that patients with HTN (T2DM+) showed worsened myocardial perfusion than those with HTN (T2DM−) and control group. A possible explanation for this may be that although hypertension and T2DM increase resting myocardial perfusion to meet increased oxygen consumption, their coexistence may amplify the abovementioned abnormalities of microvasculature that have reduced myocardial perfusion at rest.

Association between impaired myocardial perfusion and LV dysfunction

In our study, there was a significant correlation between subclinical LV systolic dysfunction and impaired myocardial perfusion, and impaired myocardial perfusion by T2DM was associated with the deterioration of subclinical LV systolic dysfunction in patients with hypertension. Our results were consistent with the study by Jiang et al. [37], which may suggest that myocardial microcirculation might be associated with myocardial systolic function, giving further support to the importance of efficient energy production in normal myocardial contraction [28]. The aggravated abnormalities of the microvasculature discussed above may compromise nutrient and oxygen delivery and energy production, impair myocardial contractility and eventually lead to LV systolic dysfunction. Therefore, pharmacologic treatment aimed at increasing myocardial microvascular function might be an effective method for improving myocardial contractility and preventing heart failure, which needs further study.

Limitation

Several limitations in this study merit comment. First, this was a cross-sectional single-center study with a relatively small sample size, and further multicenter studies with a larger population should be performed to validate our findings. Second, The PROCEED study revealed that duration of T2DM and systolic blood pressure are determinants of severity of coronary stenosis in asymptomatic diabetes [38]. Although not all our patients underwent coronary computed tomography angiography or invasive

Li *et al. Cardiovasc Diabetol*   (2020) 19:161

Page 9 of 10

coronary angiography, coronary artery disease was considered to be unlikely according to the evaluation of patients by clinical history, laboratory results, echocardiography and electrocardiography which was subsequently supported by the CMR examinations. Third, stress tests were not performed in our participants; thus, myocardial systolic function and perfusion reserve could not be evaluated, and subclinical coronary artery disease was excluded [39]. Even if subclinical coronary artery disease could not be excluded, which may subsequently cause impaired myocardial perfusion and myocardial dysfunction, our results could still reflect the impact of T2DM and hypertension after adjustment for confounders including age. Finally, follow-up observation was not conducted to examine whether changes in myocardial microcirculation over time affect myocardial structure and function, and further longitudinal studies are required to investigate the potential prognostic value of impaired myocardial perfusion and deformation in patients with coexisting hypertension and T2DM.

Conclusion

In patients with hypertension, T2DM had an additive deleterious effect on subclinical LV systolic dysfunction and myocardial perfusion. In addition, impaired myocardial perfusion by coexisting T2DM was associated with deteriorated LV systolic dysfunction, which may contribute to increased adverse outcomes.

Abbreviations
HTN: Hypertension; T2DM: Type 2 diabetes mellitus; LV: Left ventricular; CMR: Cardiac magnetic resonance; EDV: End-diastolic volume; ESV: End-systolic volume; LVEF: Left ventricular ejection fraction; LVMI: LV mass index; GRPS: Global radial peak strain; GCPS: Global circumferential peak strain; GLPS: Global longitudinal peak strain; TTM: Time to maximum signal intensity; MaxSI: Max signal intensity.

Authors' contributions
XML and LJ designed the study. XML analyzed the data and wrote the manuscript. GYK participated in the study design, data analyze, editing and review of the manuscript. YZG supervised the overall study and contributed to study design, editing and review of the manuscript. RY, PLH researched data and review the manuscript. RY, PLH, LQP, RS and WFY were responsible for collecting, sorting and statistical data. ZGY is the guarantor of this work and, as such, had full access to all the data in the study and takes responsibility for the integrity of the data and the accuracy of the data analysis. All authors read and approved the final manuscript.

Availability of data and materials
The datasets used and analyzed during the current study are available from the corresponding author on reasonable request.

Ethics approval and consent to participate
This study was approved by the Biomedical Research Ethics Committee of our Hospital, Sichuan University (Chengdu, Sichuan, China) with a waiver of informed consent due to the retrospective nature of this investigation.

Consent for publication
Not applicable.

Competing interests
The authors declare that there are no conflicts of interest.

Author details
[1] Department of Radiology, West China Hospital, Sichuan University, 37# Guo Xue Xiang, Chengdu 610041, Sichuan, People's Republic of China. [2] Department of Radiology, Sichuan Cancer Hospital and Institute, Sichuan Cancer Center, School of Medicine, University of Electronic Science and Technology of China, 55# Lan 4 RenMing Road (South), Chengdu 610041, Sichuan, People's Republic of China. [3] Department of Radiology, Key Laboratory of Birth Defects and Related Diseases of Women and Children of Ministry of Education, West China Second University Hospital, Sichuan University, 20# South Renmin Road, Chengdu 610041, Sichuan, People's Republic of China. [4] Department of Endocrinology and Metabolism, West China Hospital, Sichuan University, 37# Guo Xue Xiang, Chengdu 610041, Sichuan, People's Republic of China.

References
1. Camici PG, Crea F. Coronary Microvascular Dysfunction. N Engl J Med. 2007;356(8):830–40.
2. Climie RE, van Sloten TT, Bruno RM, Taddei S, Empana JP, Stehouwer CDA, et al. Macrovasculature and microvasculature at the crossroads between type 2 diabetes mellitus and hypertension. Hypertension. 2019;73(6):1138–49.
3. Rapsomaniki E, Timmis A, George J, Pujades-Rodriguez M, Shah AD, Denaxas S, et al. Blood pressure and incidence of twelve cardiovascular diseases: lifetime risks, healthy life-years lost, and age-specific associations in 1.25 million people. Lancet. 2014;383(9932):1899–911.
4. Tocci G, Sciarretta S, Volpe M. Development of heart failure in recent hypertension trials. J Hypertens. 2008;26(7):1477–86.
5. Chen G, McAlister FA, Walker RL, Hemmelgarn BR, Campbell NR. Cardiovascular outcomes in framingham participants with diabetes: the importance of blood pressure. Hypertension. 2011;57(5):891–7.
6. American College of Cardiology Foundation Task Force on Expert Consensus D, Hundley WG, Bluemke DA, Finn JP, Flamm SD, Fogel MA, et al. ACCF/ACR/AHA/NASCI/SCMR 2010 expert consensus document on cardiovascular magnetic resonance: a report of the American College of Cardiology Foundation Task Force on Expert Consensus Documents. Circulation. 2010;121(22):2462–508.
7. Morris DA, Otani K, Bekfani T, Takigiku K, Izumi C, Yuda S, et al. Multidirectional global left ventricular systolic function in normal subjects and patients with hypertension: multicenter evaluation. J Am Soc Echocardiogr. 2014;27(5):493–500.
8. Claus P, Omar AMS, Pedrizzetti G, Sengupta PP, Nagel E. Tissue tracking technology for assessing cardiac mechanics: principles, normal values, and clinical applications. JACC Cardiovasc Imaging. 2015;8(12):1444–60.
9. Sakuma H, Suzawa N, Ichikawa Y, Makino K, Hirano T, Kitagawa K, et al. Diagnostic accuracy of stress first-pass contrast-enhanced myocardial perfusion MRI compared with stress myocardial perfusion scintigraphy. AJR Am J Roentgenol. 2005;181(1):95–102.
10. Costa MA, Shoemaker S, Futamatsu H, Klassen C, Angiolillo DJ, Nguyen M, et al. Quantitative magnetic resonance perfusion imaging detects anatomic and physiologic coronary artery disease as measured by coronary angiography and fractional flow reserve. J Am Coll Cardiol. 2007;50(6):514–22.
11. Tadic M, Cuspidi C, Vukomanovic V, Ilic S, Obert P, Kocijancic V, et al. Layer-specific deformation of the left ventricle in uncomplicated patients with type 2 diabetes and arterial hypertension. Arch Cardiovasc Dis. 2018;111(1):17–24.

12. Mannina C, Jin Z, Russo C, Homma S, Elkind MS, Rundek T, et al. Effect of hypertension and diabetes on subclinical left ventricular systolic dysfunction in a predominantly elderly population-based cohort. Eur J Prev Cardiol. 2019:2047487319872571.

13. Wang Q, Gao Y, Tan K, Xia H, Li P. Assessment of left ventricular function by three-dimensional speckle-tracking echocardiography in well-treated type 2 diabetes patients with or without hypertension. J Clin Ultrasound. 2015;43(8):502–11.

14. Ballo P, Cameli M, Mondillo S, Giacomin E, Lisi M, Padeletti M, et al. Impact of diabetes and hypertension on left ventricular longitudinal systolic function. Diabetes Res Clin Pract. 2010;90(2):209–15.

15. Chamberlain JJ, Rhinehart AS, Shaefer CF, Neuman A. Diagnosis and management of diabetes: synopsis of the 2016 American Diabetes Association Standards of Medical Care in Diabetes. Ann Intern Med. 2016;164(8):542–52.

16. Mosteller RD. Simplified calculation of body-surface area. N Engl J Med. 1987;317(17):1098.

17. Rodrigues JC, Amadu AM, Ghosh Dastidar A, McIntyre B, Szantho GV, Lyen S, et al. ECG strain pattern in hypertension is associated with myocardial cellular expansion and diffuse interstitial fibrosis: a multi-parametric cardiac magnetic resonance study. Eur Heart J Cardiovasc Imaging. 2017;18(4):441–50.

18. Shin SM, Shim WJ, Park SM. Early changes of left ventricular function in young adults with never-treated hypertension and no left ventricular hypertrophy: relationships to ambulatory blood pressure monitoring. Clin Exp Hypertens. 2014;36(7):517–23.

19. Stylidis M, Leon DA, Rösner A, Schirmer H. Global myocardial longitudinal strain in a general population—associations with blood pressure and subclinical heart failure: The Tromsø Study. Int J Cardiovasc Imaging. 2019;36(3):459–70.

20. Liu X, Yang ZG, Gao Y, Xie LJ, Jiang L, Hu BY, et al. Left ventricular subclinical myocardial dysfunction in uncomplicated type 2 diabetes mellitus is associated with impaired myocardial perfusion: a contrast-enhanced cardiovascular magnetic resonance study. Cardiovasc Diabetol. 2018;17(1):139.

21. Vintila VD, Roberts A, Vinereanu D, Fraser AG. Progression of subclinical myocardial dysfunction in type 2 diabetes after 5 years despite improved glycemic control. Echocardiography. 2012;29(9):1045–53.

22. Leung M, Wong VW, Hudson M, Leung DY. Impact of improved glycemic control on cardiac function in type 2 diabetes mellitus. Circ Cardiovasc Imaging. 2016;9(3):e003643.

23. Rodrigues JC, Amadu AM, Dastidar AG, Szantho GV, Lyen SM, Godsave C, et al. Comprehensive characterisation of hypertensive heart disease left ventricular phenotypes. Heart. 2016;102(20):1671–9.

24. Bogdanovic J, Asanin M, Krljanac G, Lalic NM, Jotic A, Stankovic S, et al. Impact of acute hyperglycemia on layer-specific left ventricular strain in asymptomatic diabetic patients: an analysis based on two-dimensional speckle tracking echocardiography. Cardiovasc Diabetol. 2019;18(1):68.

25. Brar PC, Chun A, Fan X, Jani V, Craft M, Bhatla P, et al. Impaired myocardial deformation and ventricular vascular coupling in obese adolescents with dysglycemia. Cardiovasc Diabetol. 2019;18(1):172.

26. Sugita Y, Ito K, Sakurai S, Sakai S, Kuno S. Epicardial adipose tissue is tightly associated with exercise intolerance in patients with type 2 diabetes mellitus with asymptomatic left ventricular structural and functional abnormalities. J Diabetes Complications. 2020;34(5):107552.

27. Bilovol OM, Knyazkova II, Al-Travneh OV, Bogun MV, Berezin AE. Altered adipocytokine profile predicts early stage of left ventricular remodeling in hypertensive patients with type 2 diabetes mellitus. Diabetes Metab Syndr. 2020;14(2):109–16.

28. Miki T, Yuda S, Kouzu H, Miura T. Diabetic cardiomyopathy: pathophysiology and clinical features. Heart Fail Rev. 2013;18(2):149–66.

29. Levy BI, Schiffrin EL, Mourad J-J, Agostini D, Vicaut E, Safar ME, et al. Impaired tissue perfusion a pathology common to hypertension, obesity, and diabetes mellitus. Circulation. 2008;118(9):968–76.

30. Kozàkovà M, Palombo C, Pratali L, Pittella G, Galetta F, L'Abbate A. Mechanisms of coronary flow reserve impairment in human hypertension. An integrated approach by transthoracic and transesophageal echocardiography. Hypertension. 1997;29(2):551–9.

31. Kjaer A, Meyer C, Wachtell K, Olsen MH, Ibsen H, Opie L, et al. Positron emission tomographic evaluation of regulation of myocardial perfusion in physiological (elite athletes) and pathological (systemic hypertension) left ventricular hypertrophy. Am J Cardiol. 2005;96(12):1692–8.

32. Kawecka-Jaszcz K, Czarnecka A, Olszanecka A, Klecha A, Kwiecien-Sobstel A, Stolarz-Skrzypek K, et al. Myocardial perfusion in hypertensive patients with normal coronary angiograms. J Hypertens. 2008;26(8):1686–94.

33. Meyer C, Schwaiger M. Myocardial blood flow and glucose metabolism in diabetes mellitus. Am J Cardiol. 1997;80(3A):94A–101A.

34. Picchi A, Limbruno U, Focardi M, Cortese B, Micheli A, Boschi L, et al. Increased basal coronary blood flow as a cause of reduced coronary flow reserve in diabetic patients. Am J Physiol Heart Circ Physiol. 2011;301(6):H2279–84.

35. Sorensen MH, Bojer AS, Pontoppidan JRN, Broadbent DA, Plein S, Madsen PL, et al. Reduced myocardial perfusion reserve in type 2 diabetes is caused by increased perfusion at rest and decreased maximal perfusion during stress. Diabetes Care. 2020;43(6):1285–92.

36. Cai X, Zhang S, Deng D, Li H, Guan X, Fang J, et al. Myocardial perfusion at rest in uncomplicated type 2 diabetes patients without coronary artery disease evaluated by 320-multidetector computed tomography: a pilot study. Medicine. 2018;97(5):e9762.

37. Jiang L, Wang J, Liu X, Li ZL, Xia CC, Xie LJ, et al. The combined effects of cardiac geometry, microcirculation, and tissue characteristics on cardiac systolic and diastolic function in subclinical diabetes mellitus-related cardiomyopathy. Int J Cardiol. 2020;S0167–5273(20):33461–6.

38. Venuraju SM, Lahiri A, Jeevarethinam A, Cohen M, Darko D, Nair D, et al. Duration of type 2 diabetes mellitus and systolic blood pressure as determinants of severity of coronary stenosis and adverse events in an asymptomatic diabetic population: PROCEED study. Cardiovasc Diabetol. 2019;18(1):51.

39. Ng MY, Zhou W, Vardhanabhuti V, Lee CH, Yu EYT, Wan EYF, et al. Cardiac magnetic resonance for asymptomatic patients with type 2 diabetes and cardiovascular high risk (CATCH): a pilot study. Cardiovasc Diabetol. 2020;19(1):42.

Publisher's Note

Springer Nature remains neutral with regard to jurisdictional claims in published maps and institutional affiliations.